

Three-Dimensional Chiral Imaging by Sum-Frequency Generation

Na Ji,[†] Kai Zhang,[‡] Haw Yang,^{*,‡} and Yuen-Ron Shen^{*,†}

Department of Physics and Department of Chemistry, University of California at Berkeley, Berkeley, California 94720

Received November 15, 2005; E-mail: hawyang@berkeley.edu; yrshen@calmail.berkeley.edu

The majority of biologically important chemical species are chiral. Their functionality is often determined by their geometrical structures, which are almost always homochiral for each species: proteins are made of right-handed α -helix and left-handed β -sheets; DNA exists as right-handed double helix in stable physiological conditions.¹ The detection and characterization of chirality at both molecular and conformational levels provide important structural and functional information of biomolecules.² Visualization of the three-dimensional (3D) arrangements and placements of these molecules in cells would allow one to directly relate their conformational architectures to biological processes. An imaging technique capable of probing chirality is needed.

Optical methods have been developed to characterize chirality.³ Microscopy based on circular dichroism contrast was developed and used to obtain images of cells and inorganic chiral crystals.^{4–6} The process, however, is based on electric-dipole-forbidden interactions between molecules and light. The signal, appearing on top of a chirality-insensitive, electric-dipole-allowed background, tends to be weak and lacks sufficient contrast in microscopy. One would like to find an improved microscopic technique.

Recently, optically active sum-frequency generation (OA-SFG) was demonstrated as a sensitive spectroscopic tool to probe chirality in vibrational and electronic transitions of chiral liquids,^{7–11} thin films,¹² and even monolayers.^{9,13} Being electric-dipole-allowed and polarization-selective, it can provide good contrast in discriminating chiral objects against an achiral background, such as water in a cell, and has the potential for stain-free cellular imaging. To develop such a microscopy, however, we need to test out OA-SFG in a microscopic configuration. We report here the first study of imaging characteristics of an OA-SFG microscope using achiral micro-objects in chiral 1,1'-bi-2-naphthol (BINOL) solutions as model systems. We demonstrated optically active imaging with submicron spatial resolution and 3D sectioning capability.

The theory of OA-SFG has been described elsewhere.^{7–10} Briefly, under the electric-dipole approximation, SFG is allowed in a medium without inversion symmetry, as in the case for a chiral material. The sum-frequency (SF) signal at $\omega_{\text{SF}} = \omega_1 + \omega_2$ generated by overlapping incoming beams of frequencies ω_1 and ω_2 and intensities I_1 and I_2 in a chiral liquid is proportional to $|\chi_{\text{chiral}}^{(2)}|^2 I_1 I_2$, where $\chi_{\text{chiral}}^{(2)}$ is the nonlinear susceptibility of the chiral liquid and the beam polarizations are taken to be SPP (S-, P-, and P-polarized for ω_{SF} , ω_1 , and ω_2 waves, respectively), PSP, or PPS. $\chi_{\text{chiral}}^{(2)}$ is of opposite signs for enantiomers and is zero for racemic mixture and achiral media. With resonant enhancement,¹⁴ OA-SFG can provide chemical selectivity.^{7–11}

For OA-SFG microscopy, we used a microscope objective to focus the input beams at 415 nm (ω_1) and 830 nm (ω_2) from a Ti:sapphire laser system into a BINOL solution sandwiched between two microscope quartz slides and detected the generated SF signal

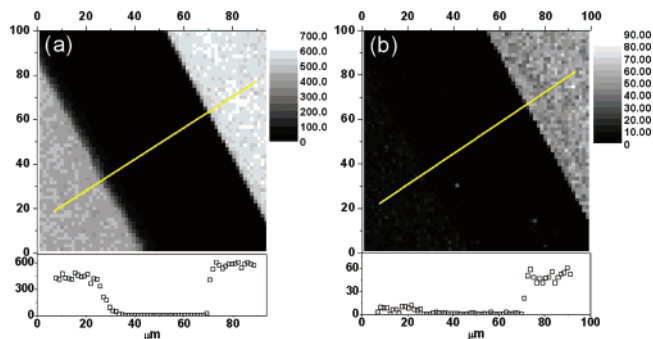


Figure 1. (a) Fluorescence image of a racemic BINOL solution and a R-BINOL solution separated by a 55 μm glass spacer. (b) OA-SFG image of the same sample measured with SPP polarization combination. Bottom panels are signal profiles along the lines in the images. The 100 μm \times 100 μm images were taken with collection times of (a) 4 ms/pixel and (b) 78 ms/pixel and power levels of 0.24 mW (ω_1) and 18 mW (ω_2).

in the transmission direction. The SF signal at 277 nm (ω_{SF}) was in resonance with an electronic transition of BINOL.¹⁵ Images taken by raster-scanning the sample stage were obtained with SPP polarization combination. (The details of our experimental setup, sample preparation, and signal characterization are described in the Supporting Information.) To demonstrate the chiral sensitivity of our SFG imaging, we prepared a sample in which an enantiomeric solution and a racemic solution of BINOL were separated by a 55 μm wide glass spacer. The microscopic image in Figure 1a was obtained by detecting fluorescence from BINOL at 350 nm. Since the fluorescence was not sensitive to chirality, both enantiomeric and racemic sections appeared bright, as shown in the figure. When the same sample was imaged by OA-SFG, only the enantiomeric section generated strong signal, as shown in Figure 1b. The achiral racemic solution did generate minimal yet detectable output at ω_{SF} , which we attribute to resonantly enhanced parametric light scattering from BINOL.¹⁶

To characterize the spatial resolution of our microscope, we imaged enantiomeric BINOL solutions sandwiched between slides decorated with 2.4 μm diameter silica beads. A reduction in signal was observed when the achiral beads were in the focal area. Two typical images, one with a single bead and the other three beads, are displayed in panels a and b of Figure 2, respectively. From the intensity profiles and the focal profile of the objective lens,¹⁷ we estimated that the lateral resolution of our microscopy was below 400 nm. This submicron resolution made it easy to resolve the three beads in Figure 2b.

As a nonlinear optical process where signal is generated only in regions with high enough intensity, OA-SFG microscopy allows 3D sectional imaging. Figure 3 presents three sectional images of a sample at different vertical positions, together with cartoons illustrating the interaction regions of light with the sample. As explained in Supporting Information, when half of the interaction

[†] Department of Physics.

[‡] Department of Chemistry.

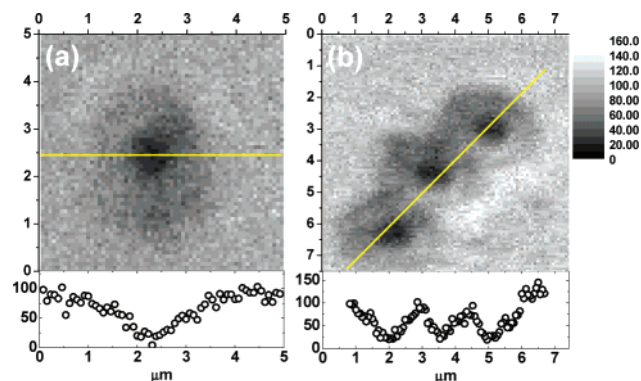


Figure 2. OA-SFG images of (a) one and (b) three $2.4 \mu\text{m}$ diameter silica beads in R-BINOL solutions. Bottom panels show signal variations along the lines in the images. The polarization combination used was SPP and the collection time per image was 78 ms/pixel at power levels of 0.18 mW (ω_1) and 14 mW (ω_2).

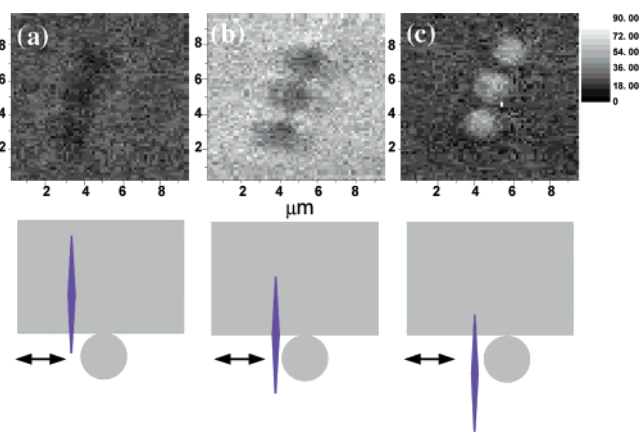


Figure 3. OA-SFG images of three $2.4 \mu\text{m}$ diameter silica beads in R-BINOL solutions with the sample at different vertical positions. Image (b) was obtained with the SFG signal from solution maximized. Images (a) and (c) were obtained with the sample vertically displaced by $+2$ and $-2 \mu\text{m}$ relative to (b), respectively. At bottom are cartoons showing the relative positions of the interaction region (blue) and the sample (gray) for fused silica slides and beads, white for R-BINOL solutions. Black arrows denote scanning direction. The polarization combination is SPP, and the collection time is 78 ms/pixel at a power of 0.24 mW (ω_1) and 18 mW (ω_2).

region is in solution, as in Figure 3b, the chiral signal was the strongest. The signal was greatly reduced if a bead appeared in the interaction region, giving rise to an image of the beads similar to those seen in Figure 2. Lowering the sample decreased the interaction volume of light with solution, and accordingly, the signal dropped sharply, as illustrated in Figure 3a (although with a much lower contrast the beads could still be resolved). Raising the sample to have the focal region well immersed in solution also sharply decreased the chiral signal from the solution, as shown in Figure 3c. This is because the SF signal generated in the focal region experienced destructive interference (see Supporting Information for detailed explanation). Scanning the focal region over the beads now enhanced the SF signal because, with part of the focal region in the bead, the total cancellation of SF signal due to destructive interference was avoided. This allowed the beads to stand out as positively contrasted objects in the image. This 3D imaging characteristic is similar to that of third harmonic generation (THG) microscopy, which has been used to obtain 3D reconstructions of biological samples.¹⁸

Just as CD is a much better tool to probe macromolecular conformation than simple absorption, OA-SFG is expected to be more sensitive to molecular conformation than existing 3D microscopic techniques.^{19,20} It also has the unique advantage that background signal from achiral species is suppressed. This makes it a potentially very useful technique for imaging biological samples. We note that Kriech et al. recently reported successful demonstration of chiral second harmonic generation (C-SHG) surface microscopy with a resolution of a few microns.²¹ This technique, however, cannot be used to probe bulk chirality because C-SHG is forbidden in isotropic chiral media. Our microscopic setup actually permits simultaneous measurements of chiral SHG and SFG from a sample and, therefore, would allow both surface and bulk chiral imaging of the same chiral system. This is important because chiral molecular arrangements and compositions at the surface and in the bulk are expected to be very different.

In summary, using chiral BINOL solutions as model systems, we have constructed the first OA-SFG microscope and demonstrated its capability to produce chirality-sensitive, 3D sectional images with submicron spatial resolution. While more research on the sensitivity and selectivity of OA-SFG to probe biological macromolecules is still needed, OA-SFG microscopy being free from achiral background has the potential to become a powerful imaging technique for biological samples.

Acknowledgment. This work was support by U.S. Department of Energy under Contract No. DE-AC03-76SF00098, and the University of California at Berkeley. The authors acknowledge the suggestion of Professor E. Schlag on possible OA-SFG microscopy at a recent conference.

Supporting Information Available: Experimental setup, sample preparation, and signal characterization. This material is available free of charge via the Internet at <http://pubs.acs.org>.

References

- Alberts, B.; Johnson, A.; Lewis, J.; Raff, M.; Roberts, K.; Walter, P. *Molecular Biology of the Cell*; Garland Publishing: New York, 2002.
- Woody, R. W. In *Biochemical Spectroscopy*; Sauer, K., Ed.; Academic Press: London, 1995; Vol. 246, p 34.
- Berova, N.; Nakanishi, K.; Woody, R. W. *Circular Dichroism: Principles and Applications*; Wiley-VCH: Weinheim, Germany, 2000.
- Maestre, M. F.; Katz, J. E. *Biopolymers* **1982**, *21*, 1899.
- Tinoco, I.; Mickols, W.; Maestre, M. F.; Bustamante, C. *Annu. Rev. Biophys. Chem.* **1987**, *16*, 319.
- Claborn, K.; Puklin-Faucher, E.; Kurimoto, M.; Kaminsky, W.; Kahr, B. *J. Am. Chem. Soc.* **2003**, *125*, 14825.
- Belkin, M. A.; Kulakov, T. A.; Ernst, K. H.; Yan, L.; Shen, Y. R. *Phys. Rev. Lett.* **2000**, *85*, 4474.
- Belkin, M. A.; Han, S. H.; Wei, X.; Shen, Y. R. *Phys. Rev. Lett.* **2001**, *87*, 113001.
- Belkin, M. A.; Shen, Y. R. *Phys. Rev. Lett.* **2003**, *91*, 213907.
- Ji, N.; Shen, Y. R. *J. Am. Chem. Soc.* **2004**, *126*, 15008.
- Ji, N.; Shen, Y. R. *J. Am. Chem. Soc.* **2005**, *127*, 12933.
- Oh-e, M.; Yokoyama, H.; Yorozuya, S.; Akagi, K.; Belkin, M. A.; Shen, Y. R. *Phys. Rev. Lett.* **2004**, *93*, 267402.
- Han, S. H.; Ji, N.; Belkin, M. A.; Shen, Y. R. *Phys. Rev. B* **2002**, *66*, 165415.
- Shen, Y. R. *The Principles of Nonlinear Optics*; John Wiley & Sons: New York, 1984.
- Hanazaki, I.; Akimoto, H. *J. Am. Chem. Soc.* **1972**, *94*, 4102.
- Verbiest, T.; Kauranen, M.; Persoons, A. *J. Chem. Phys.* **1994**, *101*, 1745.
- Muller, M.; Squier, J.; De Lange, C. A.; Brakenhoff, G. J. *J. Microsc.* **2000**, *197*, 150.
- Sun, C. K. In *Microscopy Techniques*; Rietdorf, J., Ed.; in *Advances in Biochemical Engineering/Biotechnology*; Springer-Verlag: Berlin, Heidelberg, 2005; Vol. 95, p 17.
- Barad, Y.; Eisenberg, H.; Horowitz, M.; Silberberg, Y. *Appl. Phys. Lett.* **1997**, *70*, 922.
- Zumbusch, A.; Holtom, G. R.; Xie, X. S. *Phys. Rev. Lett.* **1999**, *82*, 4142.
- Kriech, M. A.; Conboy, J. C. *J. Am. Chem. Soc.* **2005**, *127*, 2834.

JA057775Y